Multi-Scale Radio Study of the Changing-Look AGN NGC 3516

VSRP 2024
Esha Sajjanhar
Advisor: Dr. Preeti Kharb

Introduction

Active Galactic Nuclei (AGN) are active super-massive black holes (SMBH) in extremely bright galactic centres. AGN can be radio loud (RL) or radio quiet (RQ) based on whether they produce energetic jets on a large scale [1]. RL AGN show large energetic jets which can extend far outside the galaxy (several Mpc) and can outshine the total luminosity from the galaxy. On the other hand, the radio emission from RQ AGN are seen on much smaller scales (several kpc) [2]. Nearby radio-quiet AGN are known as Seyfert galaxies, while more distant AGN can be classified as QSOs. AGN can also be classified on the basis of the emission lines observed. AGN where both broad and narrow emission lines are observed are classified as type 1 whereas AGN where only narrow lines are observed are classified as type 2. Some AGN can change their types mutliple times over their lifetime. These are known as 'changing-look' AGN.

AGN are generally described by the 'unified model' shown in Figure (1). According to this model, an AGN has an accretion disk and a dusty torus surrounding a super-massive black hole (SMBH). A biconical outflow of synchrotron plasma forms radio jets or lobes around the SMBH. The broad emission lines observed are emitted by fast-moving gas near the SMBH while narrow emission lines are produced by slower gas further away from the SMBH. Based on this geometry, there are two proposed models for explaining changing-look events in AGN. The first is the 'changing obscuration' (CO) paradigm where the dusty torus is believed to be clumpy such that the presence of a dusty clump along the observer's line of sight can obscure the broad line region. The AGN is then classified as type 2 until the clump moves out of the line of sight and the AGN can again be classified as type 1. The other paradigm is the 'changing-state' (CS) paradigm wherein the accretion rate around the SMBH is variable. During low-accretion states, the intensity of line and continuum emission reduces and can thus cause the broad line to disappear [3].

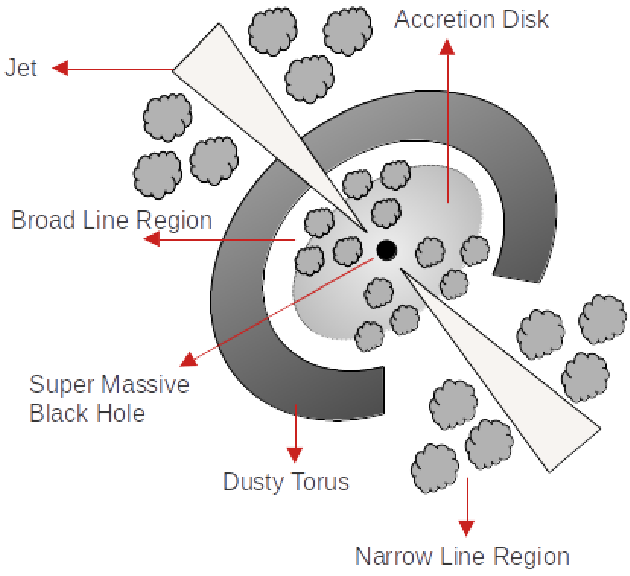

Figure 1: Schematic diagram of the unified model of AGN geometry.

NGC 3516 is a changing-look Seyfert galaxy. It is a low redshift (z=0.0088) barred spiral galaxy with an outer ring [4]. The SMBH associated with this galaxy has a mass $\sim 10^7 M_\odot$ [5]. It was originally identified as a type 1 Seyfert galaxy, but has since undergone a 'changing look (CL)' event wherein it changed its spectral type. It is now classified as a type 1.5 Seyfert galaxy. This was one of the first Seyfert galaxies to be identified and the first Seyfert source where spectral variability was detected [5]. The study of CL AGN like this one is particularly important because it allows us to understand the evolution and physics of AGN in general. This has led some campaigns for long-term multi-wavelength observation of this source in order to understand the interplay between the SMBH, the emitting region, and the host galaxy [4]. However, the radio variability of this source has never been examined.

In this project, I studied the morphology of the radio jets of this Seyfert galaxy at arcminute and arcsecond resolutions. I also examined the variability of this source to supplement existing studies of optical, UV and X-ray variability. This report is accordingly divided into two sections– morphology and variability. Each section begins with a review of the existing literature and then describes the results of this project.

1 Morphology

1.1 Literature Review

Schmitt et al (2003) performed a survey of [OIII] emission from Seyfert galaxies using the Hubble Space Telescope (HST). They find that the emission is S-shaped as shown in Figure (2a).

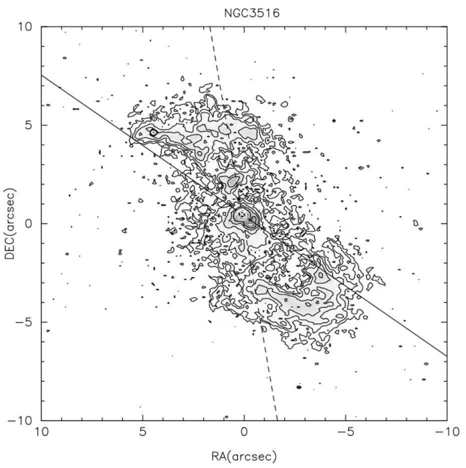

(a) [OIII] emission from NGC 3516 observed using the Hubble Space Telescope HST [6].

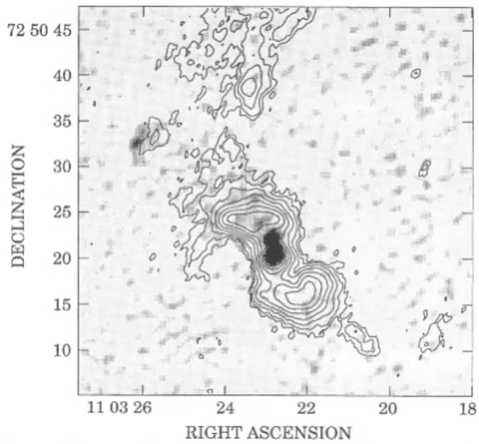

(b) [OIII] emission observed using the William Herschel Telescope (contours) with a 20cm VLA image in greyscale [7].

Figure 2: Morphology of NGC 3516 showing an S-shaped structure in both [OIII] line emission and radio plasma.

Miyaji et al. (1992) [7] present VLA (6cm, 20cm) and William Herschel Telescope observations of NGC 3516. They find a one-sided radio structure and a symmetric S-shaped structure in the optical emission lines. Their emission line maps were deeper than the HST maps and showed several fainter features as shown in Figure (2b). Notably, an emission line feature towards the North of the nucleus has no radio counterpart. The southern part of this feature seems to 'point' towards the nucleus and its peak is in good agreement with the current nuclear axis. They propose that this could be the result of ionization of ambient gas due to the active nucleus.

Veilleux et al. (1993) [8] use data from the Hawaii Imaging Fabry-Perot Interferometer (HIFI) to study the kinematics of the line emitting gas in NGC 3516. Their images confirm the features observed by [7]. They find that the line profiles in the intensity crest of the filaments to be higher than along their edges. They argue that the line emitting gas is likely to be warm outflow from the nucleus rather than ambient material ionised by other processes. They argue that the line emission originates in gas clouds entrained in the flow of the radio plasma and kept ionized by the nuclear continuum. They also point out the presence of a blueshifted emission line feature 20″ North of the nucleus which has no visible radio counterpart. This is the same feature that was detected by [7] using the WHT.

1.2 Methods

To study the morphology of this source, I used archival data from the Very Large Array (VLA) which allows us to probe kpc structure. Details of the observations used have been given in

Table (1). These data were processed using NRAO's Astronomical Image Processing Software (AIPS). The VLARUN pipeline on AIPS was used to reduce the data which were then self-calibrated. While most of the existing archival data was reduced for this project, only two representative observations have been listed here.

Project Code	Array Config	Frequency (GHz)	Date of Observation	Beam Size (Arsecond)
AW221	A	1.5	Jan, 1989	1.32 x 1.26
AB942	C	8.5	Apr, 2000	2.61 x 2.34

Table 1: Details of the VLA observations shown below.

To evaluate the results of the precession model, I wrote a Python script based on the model developed by Hjellming and Johnston (1981) [9].

1.3 Results

The contours obtained from the reduced 1.5 GHz and 8.5 GHz VLA images have been shown in Figure (3). The VLA 1.5 GHz image shows a one-sided radio structure which bends in the same direction as the emission line gas. This structure seems to show an inner core-jet structure and an initial radio jet followed by a larger radio lobe. There is a hotspot-like feature about 3.6 kpc from the core. The 8.5 GHz VLA image shows a two-sided radio structure. The counter-lobe is evidently much fainter than the lobe. This also shows the hotspot-like feature seen in the 1.5 GHz image. The total extent from the hotspot feature to the end of the counter-lobe is found to be about 7.6 kpc.

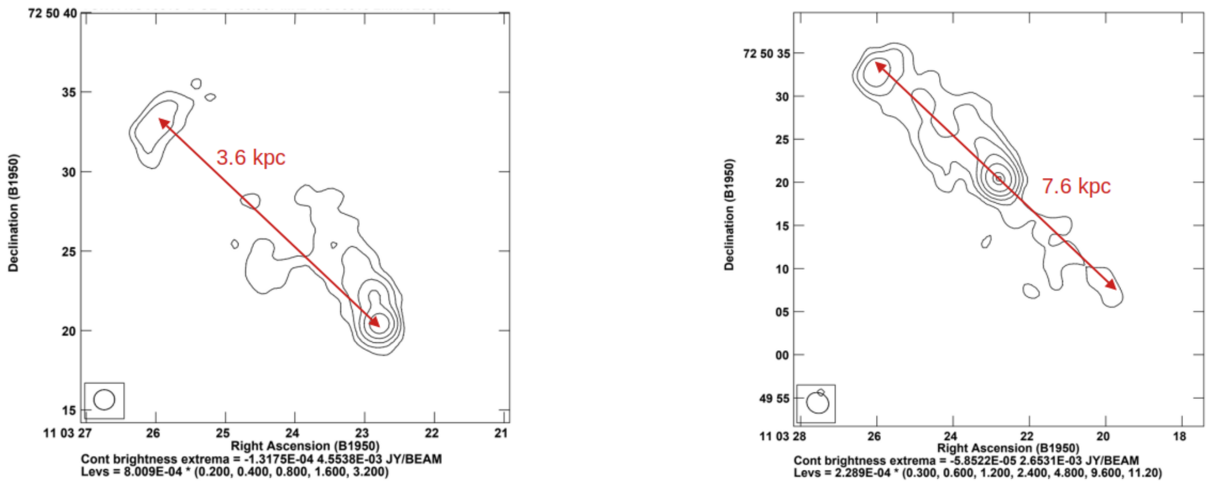

(a) Project AW221 (1.5 GHz)

(b) Project AB942 (8.5 GHz)

Figure 3: Reduced and self-calibrated VLA images showing the radio morphology and extent of the structures.

We also used equations from O'Dea and Owen (1987) [10] to compute the magnetic field in the Synchrotron plasma. They use the equipartition assumption where the magnetic field energy is equal to the total particle energy. This gave us a magnetic field of 4.82×10^{-3} mG in the lobe extending 3.6 kpc from the core. This allowed us to calculate the Synchrotron age of this lobe as 45.15 Myr using equations given by van der Laan and Perola (1969) [11]. In addition, using the flux density of the inner jet structure in the 1.5 GHz image, we can estimate the jet ejection velocity if we assume that the radio outflows are intrinsically symmetric such that the observed asymmetry is entirely due to Doppler dimming and projection effects. Then, we can use an upper limit on the counter-jet flux density (obtained using the rms noise), an assumed jet inclination, as well as the spectral index of the jet to find this value. We assume an inclination angle of 30°. Using the 1.5 GHz and 8.5 GHz data, we find an average spectral index of -0.9 for the Synchrotron plasma. These assumptions give us a jet ejection velocity of $0.48c$.

We argue that the radio plasma entrains the emission line gas which then follows the trajectory of the radio jet. This leads to the observed similarity in their morphology. The radio jet is first decelerated at the jet knot seen very close to the radio core, following this, it bends along the upper part of the bifurcation seen in the 1.5 GHz image terminating in the observed hotspot. The presence of clumpy material leads to some decollimation in this jet which then produces the lobe-like structure observed. To explain the bending of the radio jet itself, we invoke precession of the jet ejection axis. Such precession could occur due to the presence of a binary black hole system or due to a single black hole with large total angular momentum. Such a precessing jet was described by Hjellming and Johnston (1981) [9].

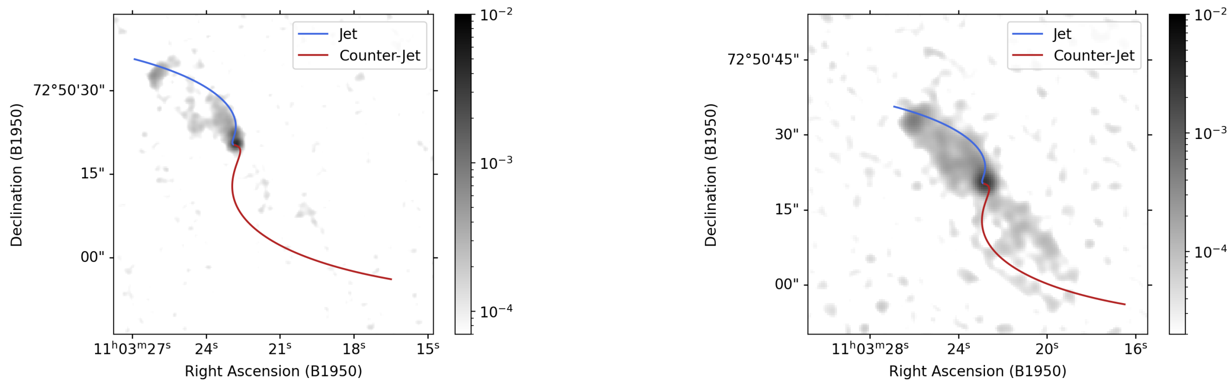

(a) Project AW221 (1.5 GHz)

(b) Project AB942 (8.5 GHz)

Figure 4: Best fit precession model overlaid on the 1.5 GHz and 8.5 GHz VLA images.

I wrote a Python-based script to evaluate the jet trajectory predicted by this model. This model takes in several parameters- opening angle of the precession cone ψ, angular velocity of precession Ω, jet inclination to the observer's line of sight i, and jet velocity in units of c, β. The constraints obtained on these parameters by fitting the model predicted trajectories to the observed morphology have been shown in Table (2). The corresponding best-fit result has been shown in Figure (4) as an overlay on each of the radio images shown above. The

Parameter	Value
i	$40° \pm 10°$
ψ	$30° \pm 15°$
θ	$40° \pm 15°$
β	$0.43° \pm 0.15°$

Table 2: Contraints obtained on the jet inclination to observer's line of sight i, opening angle of the precession cone ψ, angular velocity of precession Ω, and jet velocity in units of c, β, from the Python implementation of the precessing jet model of [9].

jet ejection velocity obtained using the ratio of jet flux density to counter-jet (limiting) flux density is found to be in agreement with the jet ejection velocity constraints obtained using the precession model.

2 Variability

Popovic et al studied the changes in the broad Hβ emission from NGC 3516 from 1996 to 2021. The observed line profiles shown in Figure (5) show a clear change in both the intensity and the shape of the broad emission. It showed a Seyfert 1 spectrum until 2014 when the broad line component decreased and almost disappeared. A weak broad line component started to reappear in 2017. In 2020-21, the broad H-beta component became stronger, perhaps indicating another CL event. An X-ray flare preceeded the increase in optical broad line profile intensity [4].

Oknyansky et al (2021) [5] reported that NGC 3516 transitioned to a bright state in 2020 and could be classified as a Sy 1.5. They report an X-ray outburst in April 2020, and prominent coronal lines. The variation of coronal lines is said to be consistent with a CL event. Popovic et al (2023) [12] proposed that CL behaviour is intrinsic to the BLR geomtery rather than due to obscuration. They argue that while the broad line starts to reappear in 2020, there are changes in the shape of the broad line which indicate that there is a change in the BLR geometry. Mehdipour et al. (2010) [13] discuss the observed variability in the X-ray spectrum and determine that it cannot be explained by varying covering fraction alone and must have significant contribution from intrinsic continuum changes. They use three phases of ionisation to model the warm absorber.

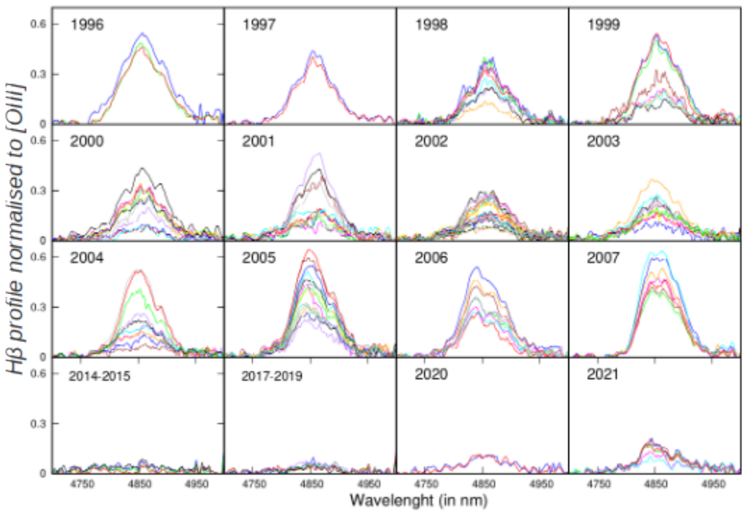

Figure 5: Hβ broad line profiles (normalised to OIII intensities) for NGC 3516 from 1996 to 2021 [12].

2.1 Methods

To study the radio variability, I used archival data from the Very Long Baseline Array (VLBA) which can resolve arcsecond structures. Details of the observations used for each telescope have been given in Table (3). These data were processed using NRAO's Astronomical Image Processing Software (AIPS). The VLBARUN pipeline was used to reduce the data.

Project Code	Frequency (GHz)	Date of Observation	Beam Size (Arsecond)	Peak Core Flux Density (mJy)
BS104	4.987	Feb, 2002	0.00431 x 0.00144	1.63
UC001D	5.68	Sept, 2020	0.00481 x 0.00200	0.76

Table 3: Details of the VLBA observations shown below.

2.2 Results

The contour maps obtained from the reduced 4.987 GHz (2002) and 5.68 GHz (2020) VLBA images have been shown in Figure (6) below. The 4.987 GHz (2002) image shows an unresolved core, while the 5.68 GHz (2020) image shows some extended emission. In addition to some diffuse emission in the North-South direction, there seems to be an extension along the East-West direction which could correspond to a new jet component being ejected from the core. The appearance of this new jet component is in keeping with the timeline of the X-ray flare observed in early 2020 [5].

As shown in Table (3), the peak core flux density in 2020 reduced to almost half of its value in

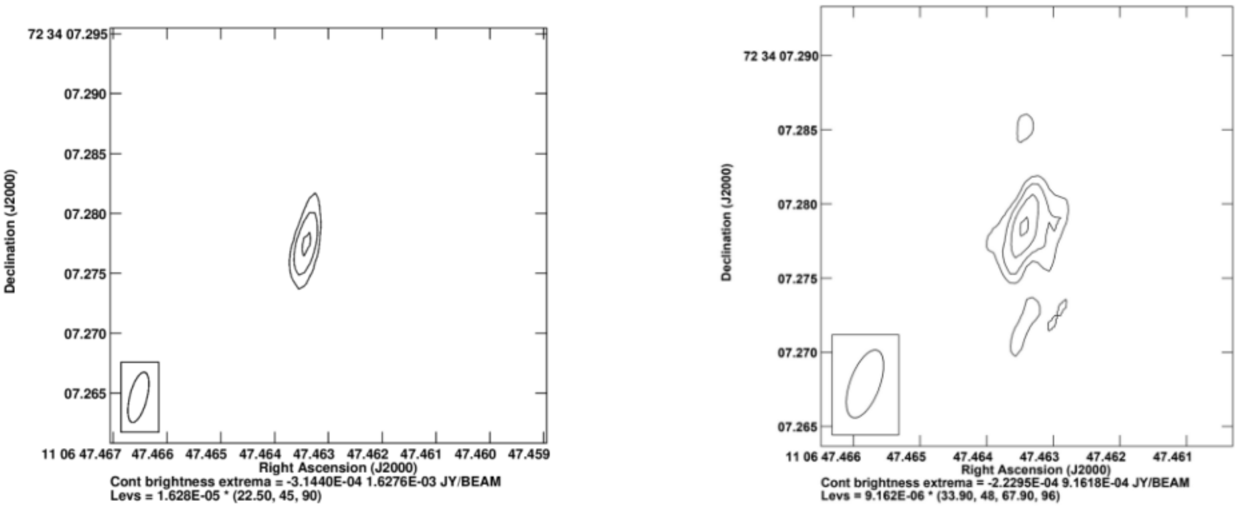

(a) Project BS104 (4.987 GHz, 2002)

(b) Project UC001D (5.68 GHz, 2020)

Figure 6: Contour plots obtained from VLBA data taken in 2002 and 2020 respectively showing the possible emergence of a new jet component in 2020.

2002. This change in the radio flux is coincident with the changes in the Hβ line profiles and the continuum flux.

Conclusions

In this project, we explored the radio morphology of NGC 3516 at multiple spatial scales and also studied its variability. It was found that the radio structure shows S-shaped morphology similar to that observed in the emission line gas, albeit at a larger scale. The S-shape of the radio jet can be well-explained by the precession of the jet ejection axis. The jet plasma entrains the emission line gas which thus follows the trajectory of the jet. The Synchrotron age of the radio lobe is found to be about 45 Myr. the counter lobe is found to be fainter than the lobe, this is understood to be a consequence of Doppler dimming and projection effects.

We also find that that the radio core of the AGN shows variability over the same timescales and in the same pattern as variability in other wavelengths. The peak flux density of the core in 2020 dims to about half of that in 2002. While the core is unresolved in 2002, it shows an inner jet-like structure in 2020. Interestingly, in April 2020, there was a flare in X-ray which was followed by an increase in the optical and UV continuum [5]. The broad line component also becomes more prominent at the same time. This indicates a relationship between broad line variability and radio variability. Further radio studies of CL AGN are needed to further understand this relationship. Such a study would allow us to distinguish between the changing obscuration and changing state models for NGC 3516. Such radio monitoring of a range of changing-look sources would allow us to better understand changing-look events.

References

[1] K. I. Kellermann et al. "VLA Observations of Objects in the Palomar Bright Quasar Survey". In: 98 (Oct. 1989), p. 1195. DOI: 10.1086/115207.

[2] Jack F. Gallimore et al. "A Survey of Kiloparsec-Scale Radio Outflows in Radio-Quiet Active Galactic Nuclei". In: *The Astronomical Journal* 132.2 (June 2006), pp. 546–569. ISSN: 1538-3881. DOI: 10.1086/504593. URL: http://dx.doi.org/10.1086/504593.

[3] Claudio Ricci and Benny Trakhtenbrot. "Changing-look active galactic nuclei". In: *Nature Astronomy* 7 (Nov. 2023), pp. 1282–1294. DOI: 10.1038/s41550-023-02108-4. arXiv: 2211.05132 [astro-ph.GA].

[4] Dragana Ilić et al. "Long-Term Optical Monitoring of Broad-Line AGNs (LoTerm AGN): Case Study of NGC 3516". In: *Physics* 6.1 (2024), pp. 31–45. ISSN: 2624-8174. DOI: 10.3390/physics6010003. URL: https://www.mdpi.com/2624-8174/6/1/3.

[5] V L Oknyansky et al. "Multiwavelength monitoring and reverberation mapping of a changing look event in the Seyfert galaxy NGC 3516". In: *Monthly Notices of the Royal Astronomical Society* 505.1 (Apr. 2021), pp. 1029–1045. ISSN: 0035-8711. DOI: 10.1093/mnras/stab1138. eprint: https://academic.oup.com/mnras/article-pdf/505/1/1029/38391819/stab1138.pdf. URL: https://doi.org/10.1093/mnras/stab1138.

[6] H. R. Schmitt et al. "A Hubble Space Telescope Survey of Extended [O III] λ5007 Å Emission in a Far-Infrared-Selected Sample of Seyfert Galaxies: Results". In: 597.2 (Nov. 2003), pp. 768–779. DOI: 10.1086/381224. arXiv: astro-ph/0307255 [astro-ph].

[7] Takamitsu Miyaji, Andrew S. Wilson, and Ismael Perez-Fournon. "The Radio Source and Bipolar Nebulosity in the Seyfert Galaxy NGC 3516". In: 385 (Jan. 1992), p. 137. DOI: 10.1086/170922.

[8] Sylvain Veilleux, R. B. Tully, and Jonathan Bland-Hawthorn. "On the Origin of the Z-Shaped Narrow-Line Region in the Seyfert Galaxy NGC 3516". In: 105 (Apr. 1993), p. 1318. DOI: 10.1086/116512.

[9] R. M. Hjellming and K. J. Johnston. "An analysis of the proper motions of SS 433 radio jets." In: 246 (June 1981), pp. L141–L145. DOI: 10.1086/183571.

[10] Christopher P. O'Dea and Frazer N. Owen. "Astrophysical Implications of the Multifrequency VLA Observations of NGC 1265". In: 316 (May 1987), p. 95. DOI: 10.1086/165182.

[11] H. van der Laan and G. C. Perola. "Aspects of Radio Galaxy Evolution". In: 3 (Dec. 1969), p. 468.

[12] Luka Č. Popović et al. "Long-term optical spectral monitoring of a changing-look active galactic nucleus NGC 3516. II. Broad-line profile variability". In: 675, A178 (July 2023), A178. DOI: 10.1051/0004-6361/202345949. arXiv: 2306.00669 [astro-ph.GA].

[13] Missagh Mehdipour et al. "Changing-look Event in NGC 3516: Continuum or Obscuration Variability?" In: *The Astrophysical Journal* 925.1 (Jan. 2022), p. 84. ISSN: 1538-4357. DOI: 10.3847/1538-4357/ac42ca. URL: http://dx.doi.org/10.3847/1538-4357/ac42ca.